Journal of Materials and Environmental Science
ISSN : 2028-2508
e-ISSN : 2737-890X
CODEN : JMESCN

J. Mater. Environ. Sci., 2022, Volume 13, Issue 06, Page 713-722

http://www.jmaterenvironsci.com

Qualitative analysis of carob fruit parts, from different Moroccan origins: FTIR-ATR approach and multivariate analysis

Aicha Akouz[1], Aziz Hasib[1]*, Bouazza Tbib[2] and Abdelali Boulli[1]

[1] *Environmental, Ecological and Agro-Industrial Engineering Laboratory, Faculty of Sciences and Technologies, Sultan Moulay Slimane University, BP 523, 23000 Beni Mellal, Morocco*

[2] *Laboratory of Nanosciences and modeling, Polydisciplinary Faculty of Khouribga, Sultan Moulay Slimane University, BP 145, 25000 Khouribga, Morocco*

**Corresponding author, Email address: azhasib@yahoo.fr*

Received 14 June 2022,
Revised 29 June 2022,
Accepted 30 June 2022

Keywords
- ✓ *Ceratonia siliqua L.*
- ✓ Chemometrics
- ✓ Discrimination
- ✓ Endosperm
- ✓ Mid-Infrared spectroscopy
- ✓ Pulp and seed

azhasib@yahoo.fr
Phone: +212662821715

Abstract

Carob fruit samples (*Ceratonia siliqua L.*) harvested from eight different regions of Morocco (Tafraout, Tiznit, Imintanoute, Ourika, El Ksiba, Imouzzer Kandar, Al Hoceima, and Chefchaouen) were subjected to qualitative analysis employing Attenuated Total Reflectance Fourier Transform Infrared Spectroscopy (FTIR-ATR) in the mid-infrared region combined with Principal Component Analysis (ACP). FTIR-ATR disclosed the major functional groups and their modes of vibration in the pulp, seed, and endosperm of each region. The peaks of the sugar region are stronger in pulp samples. However, peaks of protein region are stronger in seed and endosperm. Pulp and endosperm samples were discriminated by the ACP, while seed intersected with them. Finally, a geographical classification was carried out for each part of the carob fruit.

1. Introduction

Ceratonia siliqua L. is the scientific name of the carob tree, which is a thermophilous and dioecious evergreen species. It is well grown in subtropical and warm areas, and it tolerates the humidity of coastal areas and soils that are dry and poor [1]. Its origin according to Vavilov (1951) and De Candolle (1883) was in the eastern Mediterranean region (Turkey and Syria). Later on, it was spread to other regions in the Mediterranean basin and Mediterranean-like regions such as California, Arizona, Mexico, Chile, and Argentina [2]. In 2020, the world production of carob fruit was approximately 50 thousand tons. For the last decade, Morocco has been in the top three producers, and both its production and area harvested have increased to over 21 thousand tons and 10 thousand hectares, respectively (FAO, 2020).

The carob fruit ripens and gets dry and brown in July-August. It is a pod of 10-30 cm long and 1,5-3,5 cm wide. It is composed of 80-92 % pulp and 8-20 % seeds. Carob pulp is rich in fibers, sugars, antioxidants [3], and total polyphenols [4]. Seeds may be oval, round, or elliptic, having a smooth or rough surface. They contain antioxidants, comparatively more protein (especially arginine, aspartic

acid, and glutamic acid) than the pulp, and less sugars [1,5]. 23-25 % of the seed is the germ, 30-33% is the husk, and 42- 46% is the endosperm. This last one is rich in a polysaccharide of mannose and galactose (~ 4:1), known as carob bean gum (CBG) or locust bean gum (LBG) [1]. Carob fruit is widely used in the food industry as functional foods [6]. The carob flour can be used in the preparation of gluten-free macaron [7], roasted and used as a cocoa substitute [8], or even soaked in water to make beverages and syrup [9], and thanks to the high viscosity and gelling effect of the CBG; it is used as a food additive (stabilizer and thickener) [10].

Infrared spectroscopy (IR) is a vibrational spectroscopy based on the interaction of the sample with infrared light, which excites vibrational transitions in the molecules [11]. Fourier transform infrared spectroscopy (FTIR) uses the complete source spectrum, by dint of an interferometer that splits the radiation with a beam splitter and reflects it with two mirrors [12]. In the attenuated total reflection (ATR), the radiations reflect inside a crystal, forming evanescent waves which reach the sample on the surface [11]. The FTIR-ATR is a universal, sensitive, non-destructive, fast, and easy technique. It does not require large sample quantities or preparations [13]. Multivariate analyses are statistical techniques used to analyze a data set having multiple variables. These techniques are numerous, examples include correspondence analysis (CA), multiple correspondence analysis (MCA), multiple linear regression analysis (MLR), partial least square (PLS), discriminant analysis (DA), multiple factor analysis (MFA), and principal component analysis (PCA) [14]. This last one is the most adaptable and the oldest. It generates new uncorrelated variables resulting in maximizing the variance. Thus, with minimal information loss, the dimensionality of the data set will be reduced and the interpretability will be increased [15].

FTIR-ATR was combined with multivariate analysis for multiple purposes, such as identification and categorization of products [16,17], differentiation [18], quantification [19–22], detection of adulteration and contamination [22–24], authentication and quality assessment [25,26], qualification [21,27,28], origin identification [29], and classification and discrimination [30–32]. Alabdi et al. used the FTIR and chemometrics in 2011 to classify the seed and pod of the carob from four Moroccan regions (Essaouira, Tafraout, Fes, and Agadir) [33]. Besides, Christou et al. have adopted the same methodology to classify also the seed and pulp of carob, but from seven different countries (Palestine, Greece, Turkey, Spain, Italy, Jordan, and Cyprus) [34]. However, the carob endosperm and some other Moroccan regions had never been studied with this methodology.

In the present study, we worked on the carob pulp, seed, and endosperm harvested from eight different regions of Morocco. Aiming to analyze qualitatively its major functional groups by FTIR-ATR, and then apply the PCA to discriminate the samples regarding the part of the carob analyzed and the origin. To the best of our knowledge, the carob endosperm and some of the regions analyzed in this work were subjected -for the first time- to the FTIR-ATR spectroscopy combined with the multivariate analysis.

2. Methodology

2.1. Sample preparation

Samples of carob fruit were collected from eight different locations **(Table 1)** in Morocco: Tafraout in the central part of the Anti-Atlas, Tiznit on the southwest coast, Imintanoute and Ourika from the High-Atlas, El Ksiba and Imouzzer Kandar from the Middle-Atlas, and lastly, Al Hoceima

and Chefchaouen from the Rif's mountains in the north of the country. The rainfall data were obtained from the NASA Langley Research Center POWER [35].

For each location, samples of ten representative trees were mixed to make a representative sample of the region. The carob pods were cleaned, deseeded, and kibbled. A thermo-mechanical process separated the constituents (germ- endosperm- coat) of the seeds. Lastly, pulp, seeds, and endosperm of the carob of each location were milled and sieved to a particle size of 800 µm.

Table 1. Geographic coordinates and rainfall of the carob samples locations

Location	Code	Latitude N	Longitude W	Altitude (m)	Rainfall (mm)*
Tafraout	Taf	29º52'	9º23'	1245	214
Tiznit	Tiz	29º71'	9º72'	233	207
Imintanoute	Imi	31º17'	8º85'	1050	277
Ourika	Our	31º37'	7º80'	889	244
El Ksiba	Elk	32º58'	5º99'	1046	419
Imouzzer Kandar	Imz	33º77'	4º99'	1074	635
Al Hoceima	Alh	34º93'	3º83'	382	432
Chefchaouen	Chef	35º17'	5º27'	531	791

* Average of the last ten years

2.2. FTIR-ATR analyses of carob samples

FTIR-ATR spectra were obtained using the Perkin Elmer Spectrum Two spectrometer (PerkinElmer Inc., Waltham, Massachusetts, USA), equipped with a Lithium Tantalite ($LiTaO_3$) MIR detector and a diamond crystal cell for the attenuated total reflection (ATR). The powder of each sample was placed onto the crystal cell, at room temperature. Spectra were recorded with a resolution of 4 cm^{-1}, at 32 scans per spectrum in the range of 4000-450 cm^{-1}. The cleaning of the crystal with a tissue and isopropanol and the background collection were performed before each measurement. The average of three replicates was saved using Spectrum Software (version 10.4.2.279, PerkinElmer, Inc.).

2.3. Spectra preprocessing

Before the qualitative and multivariate analysis, some preprocessing steps were executed on the raw spectra, for the purpose of removing the noise from the random deviations of the manipulation and the systematic variations in the samples [36]. The software used was OriginPro, Version 2021 (OriginLab Corporation, Northampton, MA, USA). The first step was baseline correction using the second derivative method, which fits the bottom of the spectrum curve to the horizontal axis [37]. Then, smoothing by the Savitzky-Golay method, with 11 points of window and one order polynomial, in order to remove the noise signal [21]. Lastly, the spectra obtained were normalized to 0 to 100, this technique belongs to the scatter-correction methods, which aim to reduce the variability between samples [38].

2.4. Spectra qualitative analysis

The main bands of each spectrum were assigned to the major functional groups and their molecular vibration (torsion, bending, and stretching). This attribution is based on the band position,

and the comparison with the literature [10, 33]. 1500-450 cm^{-1} is called the fingerprint region since it is unique for every chemical structure [16]. This region contains a lot of information, however, as it is complex, it is difficult to be analyzed [13].

2.5. Multivariate analysis: principal component analysis

Principal Component Analysis (PCA) is an inferential method that evaluates the eigenvalue decomposition of the covariance matrix to reduce the dimensionality of the data set [27]. This method aims to classify and discriminate the spectra [30]. The PCA was performed on the preprocessed spectra using the PCA for spectroscopy app in the OriginPro software. The choice of the number of principal components depends on their percentage of variance and the position of the "elbow" or the "gap" in the scree plot [40]. The score plot represents the data in terms of the principal components [14].

3. Results and discussion

3.1. Spectra qualitative analysis

FTIR-ATR spectra **(Figures 1,2,3)** of the three parts of the carob fruit, harvested in eight different locations in Morocco, showed numerous peaks that could be assigned to different functional groups. Broad peaks at 3374-3208 cm^{-1} correspond to NH and OH stretching vibrations originated from carbohydrates and phenolic compounds [41]. Bands at 2927-2855 cm^{-1} reveal both the symmetrical and the asymmetrical stretching of CH_2. The region 1748-1608 cm^{-1} is assigned to C=O, and the 1730-1700 cm^{-1} peaks are attributed to its saturated stretching. Bands at 1440-1395 cm^{-1} and 960-900 cm^{-1} refer to OH in-plane and out-of-plane bandings, respectively. The 1230-1100 cm^{-1} region is assigned to the saturated C-C-C stretch. The transmission measurements observed at <1000 cm^{-1} may be due to C=C or to benzene rings [13]. The fingerprint region 1500-400 cm^{-1} provides numerous peaks attributed to bending, scissoring, stretching, torsing, and rocking vibrations [39]. This region is related to C-O and C-C stretching vibrations of carbohydrates and major sugars [23].

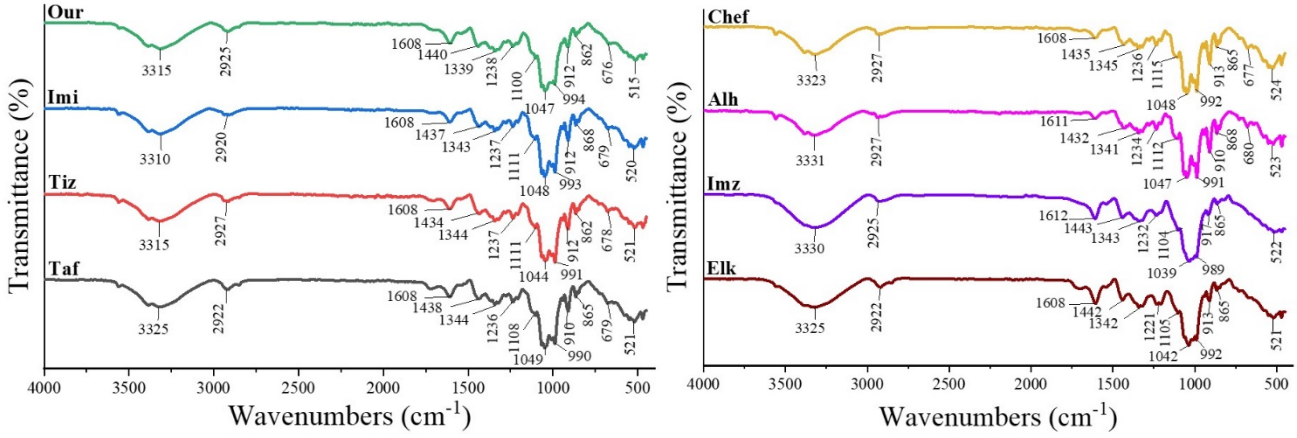

Figure 1. FTIR-ATR spectra of carob pulp samples in the mid-infrared region (4000-450 cm^{-1})

The strongest peaks in the spectra of carob *pulp* are around 1029-1027 cm^{-1} **(Figure 1)**. According to many researchers, this region is attributed to glucose [18, 19]. This finding is in accordance with the results of Li et al. who reported that peaks at wavenumbers from 1200 to 1000 cm^{-1} indicate the ether bond vibrations of the pyranose rings in sugars [42]. Peaks of this region are less broad in the spectra of the *seed* and weak in the *endosperm* spectra **(Figures 2 and 3)**.

In *seed* spectra **(Figure 2)**, bands at 2962±10 cm^{-1} and at 2872±10 cm^{-1} are assigned to asymmetric and symmetric stretches of CH_3, respectively. The strong peaks at 1570-1516 cm^{-1} correspond to NH in-plane bending [13]. Only Imintanoute, Ourika, and Al Hoceima had peaks at 3673 cm^{-1}, which corresponds to the OH vibration of alcohols and phenols [39].

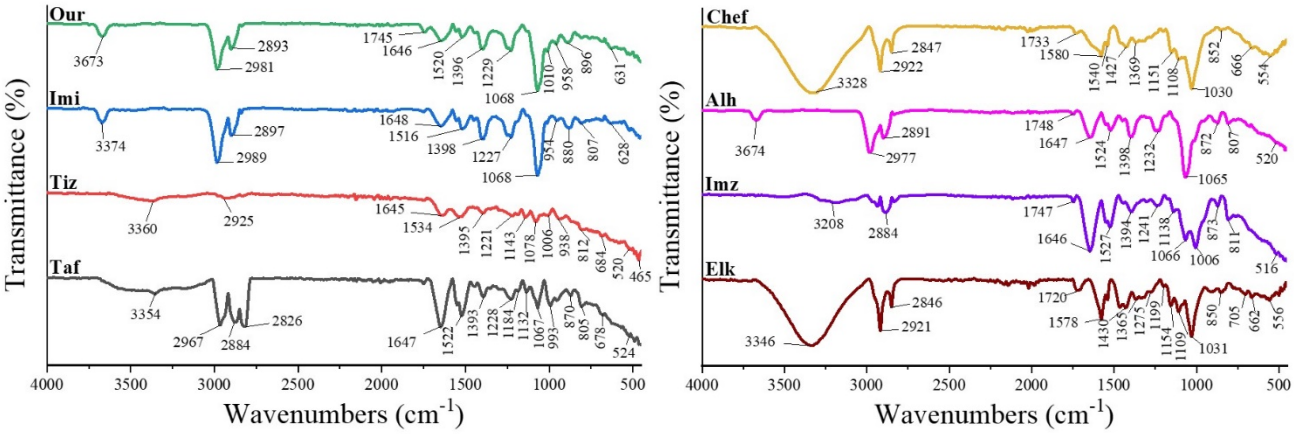

Figure 2. FTIR-ATR spectra of carob seed samples in the mid-infrared region (4000-450 cm^{-1})

The region 1641-1560 cm^{-1} in the *endosperm* spectra **(Figure 3)** contains strong and broad peaks. This region refers to the NH vibrations of primary amines and proteins [28, 33]. 1700-1600 cm^{-1} and 1531 cm^{-1} are attributed to the amide-amide-II, respectively and I. The diagnostic of the secondary structure is performed the most in the Amide-I region [43]. Surewicz et al. noticed bands at 1674, 1653, 1646, and 1631-1625 cm^{-1} revealing β-turn, α-helix, unordered, and β-sheet conformations, respectively [44]. The carob seed germ was found to have a less proportion of α-helix than β-sheet [45]. In this study, *seed* spectra had also strong peaks in this region **(Figure 2)**; however, *pulp* spectra had only weak peaks **(Figure 1)**.

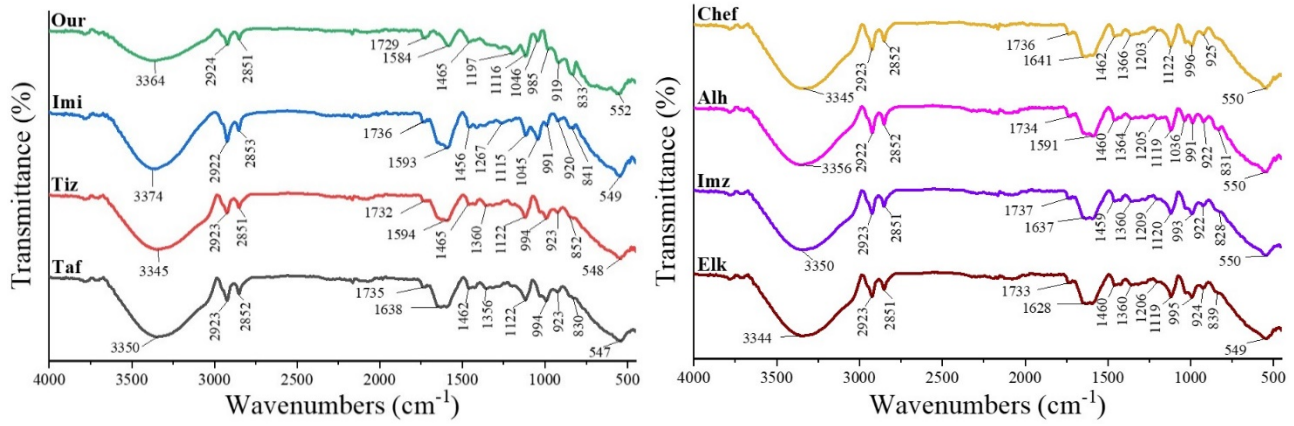

Figure 3. FTIR-ATR spectra of carob endosperm samples in the mid-infrared region (4000-450 cm^{-1})

These findings indicated that the pulp had more sugars content and less protein than the seed and the endosperm. This is consistent with results reported in the literature on the composition of carob pulp and seed [1,5]. Despite the similarities in the spectra of the eight locations, significant differences in the relative intensities were observed especially in the "fingerprint" region. Visual inspection of the spectra is not sufficient to distinguish the samples, thus, multivariate data analysis was used for better discrimination.

3.2. Multivariate analysis: principal component analysis

The principal component analysis on parts of the spectra did not present any better results, so it was performed on the full spectra (450-4000 cm^{-1}) **(Figure 4)**. The first two components explain 85.11, 82.14, 87.07, and 97.75% of the variance for the total carob samples, pulp, seed, and the endosperm spectra, respectively. The FTIR-ATR PCA model showed that the *pulp* (P) and the *endosperm* (E) samples are easily distinguished **(Figure 4 (A))**, while the *seed* (S) samples intersect with the rest of the samples. In the score plot of *pulp* samples **(Figure 4 (B))**, no geographical location classification according to both PCs was observed. Nonetheless, referring to PC1 Imintanoute and Chefchaouen appear close to each other, the same observation was made for both Ourika and Tafraout, and El Ksiba and Imouzzer Kandar. To PC2, Imintanoute. Tafraout and Chefchaouen were grouped in one group, and Imouzzer Kandar, El Ksiba, Ourika, and Al Hoceima were gathered in a second group. Three separate groups were noticed for *seed* samples **(Figure 4 (C))**, Tafraout, Tiznit, and Imouzzer Kandar in the first group. Al Hoceima, Ourika, and Imintanoute in the second. Then, Chefchaouen and El Ksiba in the third. Only one large group was observed concerning the *endosperm* samples **(Figure 4 (D))**, this group comprises Chefchaouen, El Ksiba, Tafraout, Imouzzer Kandar, Al Hoceima, and Tiznit. However, Imintanoute and Ourika were clearly separated from the rest of the origins.

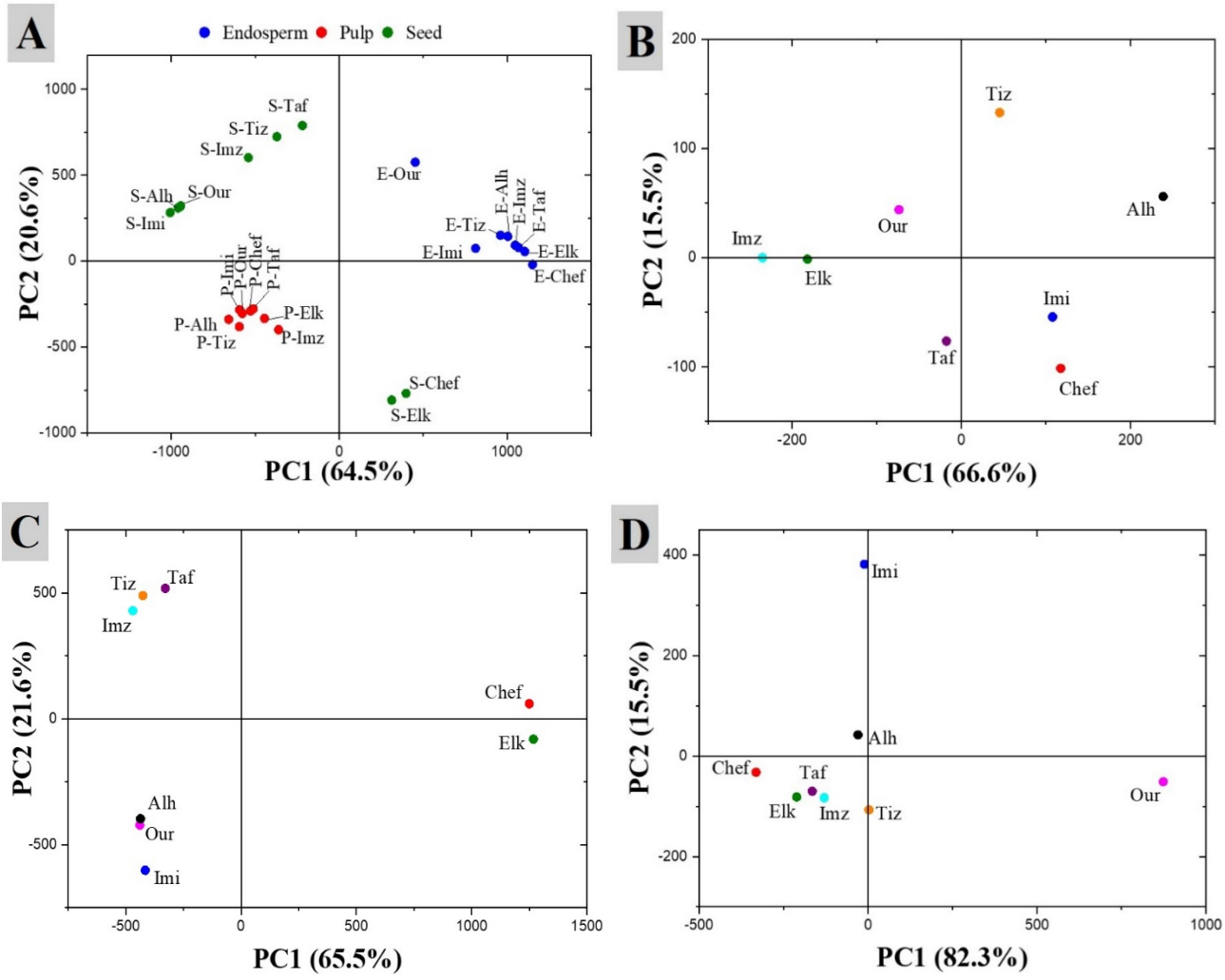

Figure 4. PCA score plots of FTIR-ATR spectra (4000-450 cm^{-1}) of (A) the total of carob samples, (B) carob pulp samples, (C) carob seed samples, and (D) carob endosperm samples

In a similar work by Christou et al., FTIR combined with PCA discriminated carob pulp and seed samples, which were originated from different countries. In the spectral range of 2500-4000 cm^{-1}, samples were classified according to their type, then the origins were separated into four groups; Cyprus, Spain, Greece, and the fourth comprised Italy, Jordan and Palestine [34].

Conclusion

In this paper, a qualitative analysis was fulfilled on three parts of carob (pulp, seed, and endosperm) harvested from eight different regions of Morocco. The FTIR-ATR spectroscopy revealed the principal functional groups in each sample. Seed and endosperm had stronger peaks than the pulp in the region of proteins, while pulp had stronger peaks in the sugars region. PCA showed that although seed intersected with other samples, pulp and endosperm samples were effortlessly separated. Lastly, a geographical differentiation was possible only on one PC at a time for pulp samples. Whereas, for the seed and the endosperm, distinct groups were distinguished on both the PCs. Consequently, we were able to analyze qualitatively and to classify both the carob endosperm and the carob collected from some Moroccan regions for the first time. As a perspective, FTIR spectroscopy might also be combined with chemometrics for the quality control and the detection of possible falsification or adulteration of carob.

Disclosure statement: *Conflict of Interest:* The authors have no conflicts of interest to disclose.
Compliance with Ethical Standards: No human or animal subjects were involved in this work.

References

[1] J. Tous, A. Romero, I. Batlle, The carob tree: botany, horticulture, and genetic resources, in: Jules Janick (Ed.), *Hortic. Rev. (Am. Soc. Hortic. Sci).*, 1st ed., John Wiley & Sons, Inc., (2013): pp. 385–454. https://doi.org/10.1002/9781118707418.ch08.

[2] I. Batlle, J. Tous, Carob tree. *Ceratonia siliqua L.*, *Int. Plant Genet. Resour. Institute, Rome, Italy.* (1997) 92.

[3] H. El Batal, A. Hasib, F. Dehbi, N. Zaki, A. Ouatmane, A. Boulli, Assessment of nutritional composition of Carob pulp (*Ceratonia Siliqua L.*) collected from various locations in Morocco, *J. Mater. Environ. Sci.* 7 (2016) 3278–3285.

[4] Z.T. Peng, Y.J. Xia, T. Yashiro, X. Gao, T.T.X. Dong, K.W.K. Tsim, H.Y. Wang, Novel phenylpropanoids and isoflavone glycoside are isolated and identified from the carob pods (*Ceratonia siliqua L.*), *Nat. Prod. Res.* (2022). https://doi.org/10.1080/14786419.2022.2076230.

[5] M. Khlifa, A. Bahloul, S. Kitane, Determination of chemical composition of carob pod (*Ceratonia siliqua L.*) and its morphological study, *J. Mater. Environ. Sci.* 4 (2013) 348–353.

[6] F.R. Saber, E.A. Mahrous, Novel Functional Foods From Plants of the Mediterranean Area: Biological, Chemical, Metabolomic Approaches, *Ref. Modul. Food Sci.* (2023). https://doi.org/10.1016/B978-0-12-823960-5.00032-9.

[7] S. Bissar, M.M. Özcan, Determination of quality parameters and gluten free macaron production from carob fruit and sorghum, *Int. J. Gastron. Food Sci.* 27 (2022) 100460. https://doi.org/10.1016/J.IJGFS.2021.100460.

[8] A. Loullis, E. Pinakoulaki, Carob as cocoa substitute: a review on composition, health benefits and food applications, *Eur. Food Res. Technol.* 244 (2017) 959–977. https://doi.org/10.1007/s00217-017-3018-8.

[9] H. El Batal, A. Hasib, A. Ouatmane, F. Dehbi, A. Jaouad, A. Boulli, Sugar composition and yield of syrup production from the pulp of Moroccan carob pods (*Ceratonia siliqua L.*), *Arab. J. Chem.* 9 (2011) S955–S959. https://doi.org/10.1016/j.arabjc.2011.10.012.
[10] F. Garcia-Ochoa, J. Casas, Viscosity of Locust Bean (*Ceratonia siliqua L.*) Gum Solutions, *J Sci Food Agric.* 59 (1992) 97–100.
[11] N. Wellner, Fourier transform infrared (FTIR) and Raman microscopy: Principles and applications to food microstructures, *Woodhead Publishing Limited*, (2013). https://doi.org/10.1533/9780857098894.1.163.
[12] F.R. van de Voort, Fourier transform infrared spectroscopy applied to food analysis, *Food Res. Int.* 25 (1992) 397–403. https://doi.org/10.1016/0963-9969(92)90115-L.
[13] B.C. Smith, Infrared Spectral Interpretation : A Systematic Approach, 1st ed., CRC Press LLC: Boca Raton, FL, USA, (1999).
[14] Hervé Abdi, Multivariate Analysis, in: *Encycl. Res. Methods Soc. Sci. Thousand Oaks Sage*, (2003): pp. 699–702.
[15] I.T. Jollife, J. Cadima, Principal component analysis: A review and recent developments, *Philos. Trans. R. Soc. A Math. Phys. Eng. Sci.* 374 (2016). https://doi.org/10.1098/rsta.2015.0202.
[16] K.Y.L. Yap, S.Y. Chan, C.S. Lim, Infrared-based protocol for the identification and categorization of ginseng and its products, *Food Res. Int.* 40 (2007) 643–652. https://doi.org/10.1016/j.foodres.2006.11.009.
[17] A. Ricci, K.J. Olejar, G.P. Parpinello, P.A. Kilmartin, A. Versari, Application of Fourier transform infrared (FTIR) spectroscopy in the characterization of tannins, *Appl. Spectrosc. Rev.* 50 (2015) 407–442. https://doi.org/10.1080/05704928.2014.1000461.
[18] B.M. Prado, S. Kim, B.F. Özen, L.J. Mauer, Differentiation of carbohydrate gums and mixtures using fourier transform infrared spectroscopy and chemometrics, *J. Agric. Food Chem.* 53 (2005) 2823–2829. https://doi.org/10.1021/jf0485537.
[19] J. Wang, T. Liu, J. Zhang, H. Yuan, G. E. Acquah, Spectral variable selection for estimation of soil organic carbon content using mid-infrared spectroscopy, *Eur. J. Soil Sci.* (2022). https://doi.org/https://doi.org/10.1111/ejss.13267.
[20] H. Lin, S.R. Bean, M. Tilley, K.H.S. Peiris, D. Brabec, Qualitative and Quantitative Analysis of Sorghum Grain Composition Including Protein and Tannins Using ATR-FTIR Spectroscopy, *Food Anal. Methods.* 14 (2020) 268–279. https://doi.org/10.1007/s12161-020-01874-5.
[21] L.M. Qi, J. Zhang, Y.L. Zhao, Z.T. Zuo, H. Jin, Y.Z. Wang, Quantitative and qualitative characterization of *Gentiana rigescens Franch (Gentianaceae)* on different parts and cultivations years by HPLC and FTIR spectroscopy, *J. Anal. Methods Chem.* (2017). https://doi.org/10.1155/2017/3194146.
[22] K.W. Se, S.K. Ghoshal, R.A. Wahab, R.K.R. Ibrahim, M.N. Lani, A simple approach for rapid detection and quantification of adulterants in stingless bees (Heterotrigona itama) honey, *Food Res. Int.* 105 (2017) 453–460. https://doi.org/10.1016/j.foodres.2017.11.012.
[23] N. Yaman, S.D. Velioglu, Use of attenuated total reflectance—Fourier transform infrared (ATR-FTIR) spectroscopy in combination with multivariate methods for the rapid determination of the adulteration of grape, carob and mulberry pekmez, *Foods*. 8 (2019). https://doi.org/10.3390/foods8070231.
[24] J. Kiefer, A.I. Lampe, S.F. Nicoli, M. Lucarini, A. Durazzo, Identification of passion fruit oil adulteration by chemometric analysis of FTIR spectra, *Molecules*. 24 (2019) 1–13. https://doi.org/10.3390/molecules24183219.
[25] K. Candoğan, E.G. Altuntas, N. İğci, Authentication and Quality Assessment of Meat Products by Fourier-Transform Infrared (FTIR) Spectroscopy, *Food Eng. Rev.* 13 (2020) 66–91. https://doi.org/10.1007/s12393-020-09251-y.
[26] L. K R Silva, L. S Santos, S. P B Ferrão, Application of infrared spectroscopic techniques to cheese authentication: A review, *Int. J. Dairy Technol.* (2022). https://doi.org/https://doi.org/10.1111/1471-0307.12859.

[27] M. Lucarini, A. Durazzo, J. Kiefer, A. Santini, G. Lombardi-Boccia, E.B. Souto, A. Romani, A. Lampe, S.F. Nicoli, P. Gabrielli, N. Bevilacqua, M. Campo, M. Morassut, F. Cecchini, Grape seeds: Chromatographic profile of fatty acids and phenolic compounds and qualitative analysis by FTIR-ATR spectroscopy, *Foods*. 9 (2020). https://doi.org/10.3390/foods9010010.
[28] V. Rizzo, F. Tomaselli, A. Gentile, S. La Malfa, E. Maccarone, Rheological properties and sugar composition of locust bean gum from different carob varieties (*Ceratonia siliqua L.*), *J. Agric. Food Chem.* 52 (2004) 7925–7930. https://doi.org/10.1021/jf0494332.
[29] Z.-Y. Cui, C.-L. Liu, D.-D. Li, Y.-Z. Wang, F.-R. Xu, Anticoagulant activity analysis and origin identification of *Panax notoginseng* using HPLC and ATR-FTIR spectroscopy, *Phytochem. Anal.* (2022) 1–11. https://doi.org/doi:10.1002/pca.3152.
[30] D. Suhandy, M. Yulia, Peaberry coffee discrimination using UV-visible spectroscopy combined with SIMCA and PLS-DA, *Int. J. Food Prop.* 20 (2017) S331–S339. https://doi.org/10.1080/10942912.2017.1296861.
[31] A. Durazzo, J. Kiefer, M. Lucarini, E. Camilli, S. Marconi, P. Gabrielli, A. Aguzzi, L. Gambelli, S. Lisciani, L. Marletta, Qualitative analysis of traditional Italian dishes: FTIR approach, *Sustain*. 10 (2018). https://doi.org/10.3390/su10114112.
[32] N. García-Gutiérrez, J. Mellado-Carretero, C. Bengoa, A. Salvador, T. Sanz, J. Wang, M. Ferrando, C. Güell, S. de Lamo-Castellví, Atr-ftir spectroscopy combined with multivariate analysis successfully discriminates raw doughs and baked 3d-printed snacks enriched with edible insect powder, *Foods*. 10 (2021). https://doi.org/10.3390/foods10081806.
[33] F. Alabdi, N. Elharfi, A. Balouki, F. Kzaiber, A. Oussama, Carob Origin Classification by FTIR Spectroscopy and Chemometrics, *J. Chem. Chem. Eng.* 5 (2011) 1020–1029. https://www.researchgate.net/publication/337104130.
[34] C. Christou, A. Agapiou, R. Kokkinofta, Use of FTIR spectroscopy and chemometrics for the classification of carobs origin, *J. Adv. Res.* 10 (2018) 1–8. https://doi.org/10.1016/j.jare.2017.12.001.
[35] A. H. Sparks, nasapower: A NASA POWER Global Meteorology, Surface Solar Energy and Climatology Data Client for R, *J. Open Source Softw.* 3 (2018) 1035. https://doi.org/10.21105/joss.01035.
[36] Å. Rinnan, Pre-processing in vibrational spectroscopy-when, why and how, *Anal. Methods.* 6 (2014) 7124–7129. https://doi.org/10.1039/c3ay42270d.
[37] Y. Jiao, Z. Li, X. Chen, S. Fei, Preprocessing methods for near-infrared spectrum calibration, *J. Chemom.* 34 (2020) 1–19. https://doi.org/10.1002/cem.3306.
[38] Å. Rinnan, F. van den Berg, S.B. Engelsen, Review of the most common pre-processing techniques for near-infrared spectra, *Trends Anal. Chem.* 28 (2009) 1201–1222. https://doi.org/10.1016/j.trac.2009.07.007.
[39] J. Coates, Interpretation of Infrared Spectra, A Practical Approach, *Encycl. Anal. Chem.* (2006) 1–23. https://doi.org/10.1002/9780470027318.a5606.
[40] M. Zhu, A. Ghodsi, Automatic dimensionality selection from the scree plot via the use of profile likelihood, *Comput. Stat. Data Anal.* 51 (2006) 918–930. https://doi.org/10.1016/j.csda.2005.09.010.
[41] A.M. Grigoriou, E. Pinakoulaki, Linking the dynamic changes in the in vitro antioxidant activity of carob kibbles upon roasting to the chemical and structural changes revealed by ftir spectroscopy, *Antioxidants*. 10 (2021). https://doi.org/10.3390/antiox10122025.
[42] R. Li, N. Tang, X. Jia, S. Nirasawa, X. Bian, P. Zhang, Y. Cheng, Isolation, physical, structural characterization and in vitro prebiotic activity of a galactomannan extracted from endosperm splits of Chinese *Sesbania cannabina* seeds, *Int. J. Biol. Macromol.* 162 (2020) 1217–1226. https://doi.org/10.1016/j.ijbiomac.2020.06.177.
[43] M. Carbonaro, A. Nucara, Secondary structure of food proteins by Fourier transform spectroscopy in the mid-infrared region, *Amino Acids.* 38 (2010) 679–690. https://doi.org/10.1007/s00726-009-0274-3.

[44] W.K. Surewicz, H.H. Mantsch, New insight into protein secondary structure from resolution-enhanced infrared spectra, *Biochim. Biophys. Acta (BBA)/Protein Struct. Mol.* 952 (1988) 115–130. https://doi.org/10.1016/0167-4838(88)90107-0

[45] G. Mamone, L. Sciammaro, S. De Caro, L. Di Stasio, F. Siano, G. Picariello, M.C. Puppo, Comparative analysis of protein composition and digestibility of *Ceratonia siliqua L.* and Prosopis spp. seed germ flour, *Food Res. Int.* 120 (2019) 188–195. https://doi.org/10.1016/j.foodres.2019.02.035.

(2022); http://www.jmaterenvironsci.com